Analytical Biochemistry 434 (2013) 105–111

Contents lists available at SciVerse ScienceDirect

Analytical Biochemistry

journal homepage: www.elsevier.com/locate/yabio

# Development of an HTS assay for EPHX2 phosphatase activity and screening of nontargeted libraries

Christophe Morisseau [a,*], Sunil Sahdeo [b], Gino Cortopassi [b], Bruce D. Hammock [a]

[a] Department of Entomology and UCD Comprehensive Cancer Center, CA 95616, USA
[b] Department of Molecular Biosciences, School of Veterinary Medicine, University of California at Davis, Davis, CA 95616, USA

ARTICLE INFO

*Article history:*
Received 6 September 2012
Received in revised form 13 November 2012
Accepted 22 November 2012
Available online 3 December 2012

*Keywords:*
Soluble epoxide hydrolase
HTS assay
Phosphatase
Ebselen

ABSTRACT

The EPXH2 gene encodes soluble epoxide hydrolase (sEH), which has two distinct enzyme activities: epoxide hydrolase (Cterm-EH) and phosphatase (Nterm-phos). The Cterm-EH is involved in the metabolism of arachidonic acid epoxides that play important roles in blood pressure, cell growth, inflammation, and pain. While recent findings suggested complementary biological roles for Nterm-phos, research is limited by the lack of potent bioavailable inhibitors of this phosphatase activity. Also, a potent bioavailable inhibitor of this activity could be important in the development of therapy for cardiovascular diseases. We report herein the development of an HTS enzyme-based assay for Nterm-phos ($Z' > 0.9$) using AttoPhos as the substrate. This assay was used to screen a wide variety of chemical entities, including a library of known drugs that have reached through clinical evaluation (Pharmakon 1600), as well as a library of pesticides and environmental toxins. We discovered that ebselen inhibits sEH phosphatase activity. Ebselen binds to the N-terminal domain of sEH ($K_I = 550$ nM) and chemically reacts with the enzyme to quickly and irreversibly inhibit Nterm-phos, and subsequently Cterm-EH, and thus represents a new class of sEH inhibitor.



In mammals, The EPHX2 gene encodes the soluble epoxide hydrolase (sEH), a cytosolic enzyme ubiquitous in vertebrates [1]. While highly expressed in the liver, sEH is also expressed in other tissues including vascular endothelium, leukocytes, red blood cells, smooth muscle cells, adipocytes, and the proximal tubule [1–3]. The sEH protein is a homodimer with a monomeric unit mass of 62.5 kDa [4]. Interestingly, sEH has two distinct activities in two separate structural domains of each monomer: the C-terminal epoxide hydrolase activity (Cterm-EH; EC 3.3.2.10) and the N-terminal phosphatase activity (Nterm-phos; EC 3.1.3.76) [4]. The Cterm-EH is responsible for the biological roles associated with sEH [1,2,5–7], while a magnesium-dependent hydrolysis of phosphate esters is associated with the Nterm-phos [8,9]. The Cterm-EH hydrolyzes epoxy-fatty acids such as epoxyeicosatrienoic acids that are potent endogenous signaling molecules [10]. Through the development of potent selective inhibitors, we demonstrated the Cterm-EH to be a novel pharmacological target to treat hypertension, inflammation, and pain in animal models [5–7,11], Pharmacological inhibition of Cterm-EH has resulted in anti-inflammatory [5,6], anti-hypertensive [12,13], neuroprotective [14], and cardioprotective effects [5].

Although the role of the Nterm-phos activity is not known, recent findings suggest a biological role. The sEH-null mice that lack both Cterm-EH and Nterm-phos activities have lower cholesterol and steroid levels [15]. Furthermore, in recombinant HepG2 cells, Cterm-EH activity lowered cholesterol synthesis while Nterm-phos activity increased it [16]. Taken together, these data suggest that sEH regulates cholesterol levels in vivo and in vitro and that the Nterm-phos is a potential therapeutic target in hypercholesterolemia-related disorders. Similarly, in recombinant endothelial cells, both Cterm-EH and Nterm-phos activities contribute to growth factor expression and cell growth [17]. In mice, it seems that the Nterm-phos may play a role in the development of hypoxia-induced pulmonary hypertension [18]. The phosphatase activity of sEH was shown recently to play a pivotal role in the regulation of endothelial nitric oxide (NO) synthase activity and NO-mediated endothelial cell functions [19]. Human polymorphism studies have shown that the Arg287Gln polymorph of sEH is associated with the onset of coronary artery calcification in African-American subjects [20] and insulin resistance in type 2 diabetic patients [21]. This single-nucleotide polymorphism (SNP G860A) of sEH reduces both Cterm-EH and Nterm-phos activities [22,23]. Furthermore, people having a Lys55Arg polymorphism of sEH, which has reduced Nterm-phos but increased Cterm-EH, have higher risk of coronary heart diseases. The presence of this SNP also increases the long-term risk of ischemic stroke in men [24]. In support of a role for

* Corresponding author. Fax: +1 (530) 751 1537.
*E-mail address:* chmorisseau@ucdavis.edu (C. Morisseau).

0003-2697/$ - see front matter © 2012 Elsevier Inc. All rights reserved.
http://dx.doi.org/10.1016/j.ab.2012.11.017

Nterm-phos in these processes, sEH phosphatase activity was recently shown to represent a significant part of cellular lysophosphatidic acid hydrolysis in various tissues [25].

Specific catalytic enzyme inhibitors are important research tools to help understand the mechanism of an enzyme and of pathologies that may be associated with dysfunctions of this enzyme. A potent bioavailable inhibitor of this activity could also be important as a potential therapeutic in some cardiovascular diseases. Because common commercial phosphatase inhibitors do not influence the Nterm-phos activity [9], it is necessary to develop new phosphatase inhibitors for Nterm-phos as biochemical and physiological probes. We recently developed the first generation of Nterm-phos inhibitors. While sulfates were shown not to be Nterm-phos substrates [8], we described sulfate, sulfonate, and phosphonate lipids as novel potent inhibitors of Nterm-phos [26]. These compounds are competitive inhibitors with inhibition constant ($K_I$) values in the low-micromolar range. They act by mimicking the binding of the phosphate substrate in the catalytic cavity [26]. Farnesyl derivatives were also shown to inhibit Nterm-phos in the micromolar range by chelating the catalytic magnesium ion [27,28]. While these inhibitors are effective in vitro, they have limited efficacy in cell cultures, and they are completely inactive in vivo. These results highlight the need to improve the potency of Nterm-phos inhibitors as well as their availability. To achieve this goal, we report herein the development of an HTS assay for Nterm-phos and the screening of two chemical libraries containing a wide variety of chemical entities: a 176-synthetic-chemical library of mostly pesticides [29] and another library of 1600 known drugs from the U.S. and International Pharmacopeia (Pharmakon 1600).

## Materials and methods

### *Materials*

The environmental chemical library was prepared previously in the laboratory [29]. The Pharmakon 1600 library of chemicals was obtained from Microsource Discovery Systems (Gaylordsville, CT, USA). The AttoPhos substrate was obtained from Promega (Madison, WI, USA). All chemicals and solvents were obtained from Fisher Scientific (Pittsburgh, PA, USA) or Sigma–Aldrich (St. Louis, MO, USA) and were used without further purification.

### *Enzyme preparations*

Recombinant human sEH (HsEH) was produced in a baculovirus expression system [30], and purified by affinity chromatography [31]. This enzyme preparation was at least 97% pure, based on SDS–PAGE followed by scanning densitometry. The enzyme preparation was kept at −80 °C until usage. Protein concentration was quantified by using the Pierce BCA assay using fraction V bovine serum albumin (BSA) as the calibrating standard.

### *Optimization of assay conditions*

To optimize enzyme and substrate concentrations, a checkerboard assay was carried out, which tested combinations of several final concentrations of substrate (AttoPhos, 12.5–100 μM) and serial dilutions of enzyme (HsEH, 1.6–105 nM, 0.02–1.31 μg/well, 200 μl/well) in BisTris–HCl buffer (25 mM, pH 7.0), containing 1 mM $MgCl_2$ and 0.1 mg/ml BSA (buffer A). BSA was used to stabilize the human sEH and to reduce nonspecific inhibition [29]. The progress of the reaction was followed by measuring the appearance of the fluorescent alcohol ($\lambda_{ex}$ 435 nm, $\lambda_{em}$ 555 nm, $\lambda_{cutoff}$ 515 nm) using a SpectraMax M2 microplate reader (Molecular Devices, Sunnyvale, CA, USA) at room temperature (23 °C) with reads every 3 min for 2 h. Each condition was done in triplicate.

Several chemicals and solvents were tested for their ability to stop the Nterm-phos enzymatic reaction for a fluorescence endpoint measurement setting. These chemicals and solvents were examined for their ability to prohibit enzyme reaction and substrate autohydrolysis, as well as to maintain the existing fluorescent signal. Reactions were conducted using optimized assay conditions ($[E]_{final}$ 2.1 nM; $[S]_{final}$ 25 μM). After a 60-min incubation at room temperature in the dark, 100 μl of stop solution was added to each well; buffer A was added in the control wells. After the addition of candidate stop solutions, we tested their efficacy at stopping the reaction and effects on the fluorescent signal strength and stability by measuring the fluorescence ($\lambda_{ex}$ 435 nm, $\lambda_{em}$ 555 nm, $\lambda_{cutoff}$ 515 nm) every 5 min for 30 min at room temperature (23 °C). Each condition was done in 16 replicates. Hydrolysis rates were determined by linear regression analyses employing the plate reader's software (SoftMax Pro 4.7). The signal-to-background ratio ($S/B$) was calculated by dividing the reaction average velocity in the presence of enzyme ($Ave_{enz}$) by the average background hydrolysis rate ($Ave_{blank}$). The signal-to-noise ratio ($S/N$) was calculated by dividing the reaction velocity in the presence of enzyme by the standard deviation of the background hydrolysis ($SD_{blank}$). The $Z'$ factor was calculated following the method of Zhang et al. [32] using the formula $Z' = 1 - ([3 \times (S_{Denz} + SD_{blank})]/(Ave_{enz} - Ave_{blank}))$.

### *Assay validation for inhibition study, interplate variation, and accuracy*

Assay validation for the endpoint assay system was performed. To a black polystyrene 96-well plate, 150 μl of buffer A was added to each well. Two microliters of inhibitor solution in dimethyl sulfoxide ($Me_2SO$) was then added to 3 wells for each concentration ($0.8 < [I]_{final} < 100$ μM); 2 μl of carrier solvent only was added to the 100% activity control wells. Then, 20 μl of a 21 nM solution of HsEH in buffer A was added to the wells ($[E]_{final}$ 2.1 nM); for the background hydrolysis wells, the enzyme was replaced by 20 μl of buffer A. After thorough mixing and preincubation at room temperature for 5 min, the reaction was started by the addition of 30 μl of a 167 μM solution of AttoPhos in buffer A ($[S]_{final}$ 25 μM). After 60 min incubation at room temperature in the dark, 100 μl of 0.1 M NaOH in water was added to each well. After strong mixing, the progress of the reaction was measured as described above. Measurement of three plates testing three inhibitors, in ABC, BCA, and CAB order, was repeated three times on three separate days, using different solutions of enzyme, inhibitors, and substrate each time.

### *Assay in 384-well plate*

To a black polystyrene 384-well plate, 37.5 μl of buffer A was added to each well. One microliter of inhibitor solution in $Me_2SO$ was then added to 3 wells for each concentration ($0.8 < [I]_{final} < 100$ μM); 1 μl of carrier solvent only was added to the 100% activity control wells. Then, 5 μl of a 21 nM solution of HsEH in buffer A was added to the wells ($[E]_{final}$ 2.1 nM); for the background hydrolysis wells, the enzyme was replaced by 5 μl of buffer A. After thorough mixing and preincubation at room temperature for 5 min, the reaction was started with the addition of 7.5 μl of a 166.7 μM solution of AttoPhos in buffer A ($[S]_{final}$ 25 μM). After 60 min incubation at room temperature in the dark, 25 μl of 0.1 M NaOH in water was added to each well. After strong mixing, the progress of the reaction was measured as described above.

*Library screening*

We used a small library of 176 compounds distributed on two 96-well plates (88 chemicals dissolved at 10 mM in $Me_2SO$ per plate, plus 8 wells containing only $Me_2SO$ for control and blank) and a 1600-compound library distributed over 20 plates (80 compounds dissolved in 10 mM in $Me_2SO$ per plate, plus 16 wells containing only $Me_2SO$ for control and blank). The inhibitors were diluted down to 100 μM by 10-fold increments in buffer A. In a black polystyrene 96-well plate, 20 μl of the inhibitor solution was delivered to every well ($[I]_{final}$ 10 μM). Then, 150 μl of a 2.8 nM solution of HsEH in buffer A was added to the wells ($[E]_{final}$ 2.1 nM); for the background hydrolysis wells, the enzyme was replaced by 150 μl of buffer A. After thorough mixing and preincubation at room temperature for 5 min, the reaction was started by the addition of 30 μl of a 167 μM solution of AttoPhos in buffer A ($[S]_{final}$ 25 μM). After 60 min incubation at room temperature in the dark, 100 μl of 0.1 M NaOH in water was added to each well. After strong mixing, the amount of fluorescent alcohol produced was measured as described above. Compounds that gave more than 80% inhibition at 10 μM were selected as positive hits, because the fluorescent signal observed for them was not significantly different from the signal for 100% inhibition. For counterscreening, fresh solutions of all positive compounds were prepared in $Me_2SO$. The $IC_{50}$ for each compound (i.e., the concentration of an inhibitor that inhibited 50% of the enzyme activity) was determined by measuring Nterm-phos activities in the absence and presence of increasing concentrations of inhibitor ($0.1 < [I] < 10$ μM) using AttoPhos as substrate in a kinetic setup as described [26]. $IC_{50}$ was calculated by nonlinear regression of at least five data points using SigmaPlot. Results are means ± standard deviation of at least three separate measurements.

## Results and discussion

*Optimization of HTS assay*

AttoPhos was previously shown to be a good fluorescent substrate for sEH phosphatase activity [26]. Prior to using this substrate for a screening assay, we first tested the effects of enzyme and substrate concentrations and time on the assay performances. Although measurements were obtained for up to 120 min, at time = 60 min (a common HTS assay endpoint), we calculated for each condition the linearity of the reaction ($r^2$), the percentage of substrate turnover (%TO), the *S/B*, the *S/N*, and the *Z′* factor (Table 1 and Supplementary Fig. S1). Linear ($r^2 > 0.99$) increases in fluorescence were observed for [E] ⩽6.6 nM, at all the [S] tested, and this increase stayed linear for up to 2 h (Fig. 1). The best results were obtained for [S] ⩾ 25 μM and [E] < 3.3 nM. Under such conditions, less than 5% of the initial substrate is consumed. However, for the higher [S] (50 and 100 μM) the *S/B* and *S/N* ratios decreased, because the background hydrolysis rate increased while the enzymatic rate did not change, as expected, because we were under saturation conditions ($[S] > 5 \times KM$). For the lowest [E], the *S/B* and *S/N* ratios decreased. Thus, the best conditions are [S] 25 μM and $1 \leqslant [E] \leqslant 6.6$ nM. For screening of libraries we used [E] 2.1 nM.

The search for an appropriate stop solution was then carried out to increase flexibility of the fluorescence endpoint assay for Nterm-phos. If it were possible to stop an ongoing substrate hydrolysis reaction and conserve the current signal, the endpoint assay could potentially be interrupted any time between 60 and 90 min after substrate addition. Most importantly, the quantification of the fluorescent signal could be achieved independent of the assay starting time, which would significantly improve the adaptability of the system. Three kinds of conditions were tested: addition of cosolvent to denature the enzyme (i.e., methanol, ethanol), addition of selective Nterm-phos inhibitor [26], and change to a pH at which Nterm-phos is inactive. As seen in Table 2, addition of methanol and ethanol reduced significantly the enzymatic hydrolysis rate as well as the fluorescence signal, thus decreasing the assay performance. The alkalization of the reaction with NaOH completely stopped the reaction at pH values above 10. Furthermore, the fluorescent signal was increased by an order of magnitude; this is probably due to the formation of the fluorescent phenolate (Supplementary Fig. S2). It resulted in higher *S/B* and *S/N* ratios as well as higher *Z′* factors. As seen in Supplementary Fig. S3, the increase in fluorescence by 0.1 M NaOH is proportional ($r^2 > 0.99$) to the fluorescence resulting from the enzymatic activity at pH 7.0. Interestingly, the addition of a high concentration of SDS (10 mM), a low-nanomolar Nterm-phos inhibitor [26], resulted in complete loss of the fluorescent signal. At such high concentrations, SDS forms micelles that could quench the fluorescent signal.

**Table 1**
Results of the checkerboard assay for the optimization of [E] and [S] after 60 min of reaction at room temperature.

| [E] (nM) | [S] (μM) | | | |
|---|---|---|---|---|
| | 12.5 | 25 | 50 | 100 |
| 105.0 | | | | |
| $r^2$ | 0.006 | 0.151 | 0.028 | 0.048 |
| %TO | 100 | 100 | 100 | 100 |
| *S/B* | 199 | 65 | 40 | 29 |
| *S/N* | 671 | 918 | 215 | 352 |
| *Z′* | 0.81 | 0.85 | 0.89 | 0.96 |
| 52.5 | | | | |
| $r^2$ | 0.365 | 0.213 | 0.325 | 0.412 |
| %TO | 100 | 100 | 65 | 43 |
| *S/B* | 179 | 79 | 35 | 16 |
| *S/N* | 611 | 1123 | 186 | 190 |
| *Z′* | 0.95 | 0.91 | 0.93 | 0.84 |
| 26.2 | | | | |
| $r^2$ | 0.835 | 0.734 | 0.912 | 0.935 |
| %TO | 100 | 48 | 25 | 13 |
| *S/B* | 190 | 57 | 26 | 19 |
| *S/N* | 646 | 802 | 137 | 225 |
| *Z′* | 0.95 | 0.79 | 0.78 | 0.85 |
| 13.1 | | | | |
| $r^2$ | 0.98 | 0.908 | 0.989 | 0.986 |
| %TO | 45 | 26 | 12 | 5 |
| *S/B* | 143 | 60 | 49 | 33 |
| *S/N* | 488 | 856 | 262 | 393 |
| *Z′* | 0.89 | 0.83 | 0.84 | 0.85 |
| 6.6 | | | | |
| $r^2$ | 0.999 | 0.999 | 0.999 | 0.999 |
| %TO | 28 | 13 | 6 | 3 |
| *S/B* | 89 | 52 | 31 | 18 |
| *S/N* | 305 | 730 | 165 | 216 |
| *Z′* | 0.82 | 0.88 | 0.81 | 0.66 |
| 3.3 | | | | |
| $r^2$ | 0.998 | 0.999 | 0.999 | 0.999 |
| %TO | 15 | 6 | 3 | 2 |
| *S/B* | 48 | 26 | 16 | 9 |
| *S/N* | 162 | 370 | 84 | 107 |
| *Z′* | 0.87 | 0.91 | 0.74 | 0.88 |
| 1.6 | | | | |
| $r^2$ | 0.998 | 0.999 | 0.999 | 0.999 |
| %TO | 8 | 4 | 2 | 1 |
| *S/B* | 25 | 15 | 8 | 5 |
| *S/N* | 86 | 206 | 42 | 60 |
| *Z′* | 0.87 | 0.78 | 0.80 | 0.85 |
| 0 | | | | |
| $r^2$ | 0.055 | 0.083 | 0.214 | 0.333 |
| %TO | <1 | <1 | <1 | <1 |

%TO, percentage of substrate turnover.

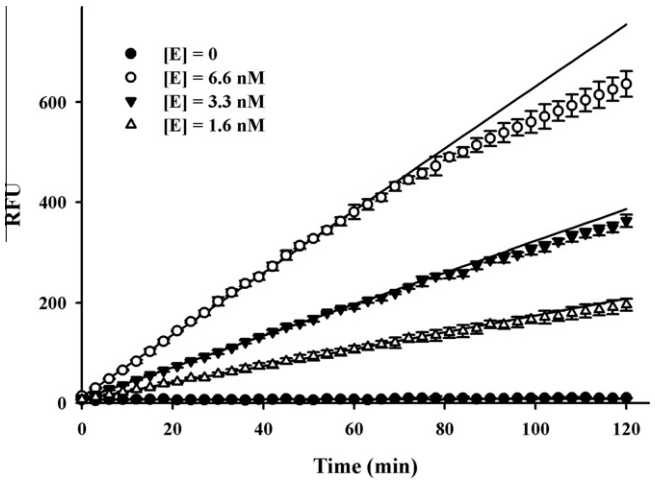


**Fig.1.** Time course analysis of the hydrolysis of 25 μM AttoPhos by various concentrations of human sEH. The lines are the regression for the first 60 min of the reaction.

*Assay validation*

To validate the assay, we first investigated its ability to differentiate between and classify known inhibitors of various potencies. The $IC_{50}$ values of previously characterized sEH inhibitors were determined employing the endpoint assay system described above. Using a kinetic assay [26], dodecyl phosphate was found to be a better inhibitor than dodecyl sulfonate or dodecyl sulfate (Table 3). In a second experiment, we tested the repeatability of the assay by measuring its accuracy and precision by measuring the inhibition of three inhibitors over several plates (three plates/day) and several days (3 days total). Overall, we found less than 5% variation in the assay performance (Table 3). For inhibition above 20%, we obtained accuracy above 95% and a variation in precision under 5%. This results in less than 10% variation in the calculated $IC_{50}$. Results for each day were very similar. When looking at the difference in signal between inhibited and uninhibited enzyme samples, a significant separation of the signals ($Z$ values >0.6) was obtained for inhibition below 80% (Supplementary Fig. S4). Put together, these data indicate that the assay is highly reproducible and accurate, with a good separation and signal-to-noise ratio between inhibition of 20% and 80%. Accuracy decreased below 20%, and above 80% the signal was not statistically discernible from the background. Finally, we tested the performance of the assay in a 384-well format. As shown in Supplementary Table S1, overall, larger variations were obtained but the results obtained from 384-well plates were similar to those from 96-well plates in terms of assay performance ($S/B$, $S/N$, and $Z'$) and ability to measure accurately inhibitor potency. The assay performance could probably be improved further by robotic addition of reagents.

*Library screening*

To test the ability of the assay to select new chemical entities that potently inhibit Nterm-phos, we first screened a small library of pesticides [29] at two final concentrations of the tested chemicals (1 and 10 μM). Overall, we obtained $S/B = 170 \pm 17$, $S/N = 1180 \pm 120$, and $Z' = 0.92 \pm 0.02$, indicating that the assay performed very well. Of 176 compounds, 3 compounds gave more than 50% inhibition at 10 μM and only 1 of them at 1 μM. This most potent compound was identified as dodecyl phosphoric acid, a known Nterm-phos inhibitor (see above) with an $IC_{50}$ of 2.2 ± 0.3 μM, confirming the ability of the assay to discriminate sEH phosphatase inhibitors, and to discover new structures that inhibit Nterm-phos, one should screen at 10 μM [33]. The potencies of the 2 other positive compounds, Folpet and Nabam, were tested using freshly made solutions. Nabam was found not to significantly inhibit Nterm-phos ($IC_{50}$ > 100 μM), while Folpet yielded an $IC_{50}$ of 25 ± 3 μM.

A library of 1600 commercial drugs was then screened at a final concentration of 10 μM, following the method described above. Overall, we obtained on average for the 20 plates $S/B = 55 \pm 10$, $S/N = 840 \pm 210$, and $Z' = 0.92 \pm 0.03$, indicating that the assay performed very well. Of 1600 compounds, 24 (1.5%) inhibited Nterm-phos by over 50% at 10 μM, and 9 of these inhibited the enzyme by over 80% (Supplementary Fig. S5). The 24 compounds were retested, but using the AttoPhos assay in kinetic mode to eliminate compounds that affect the fluorescent signal. Only 6 compounds were found to give more than 80% inhibition. The potencies of these 6 positive compounds were then measured using freshly made solutions (Table 4). Only 2 compounds (ebselen and sodium tetradecyl sulfate) were found to significantly inhibit Nterm-phos. Because sodium tetradecyl sulfate is a detergent, its inhibition of Nterm-phos could be due to a nonspecific promiscuous effect. However, sodium tetradecyl sulfate (STS) critical micelle concentration is around 2 mM [34], roughly 100-fold higher than the concentrations at which we observed Nterm-phos. Thus, it is unlikely that Nterm-phos inhibition by STS is not specific. Furthermore, we previously showed that alkyl sulfates are competitive inhibitors of the sEH phosphatase activity [26]; thus one could expect that sodium tetradecyl sulfate inhibits Nterm-phos in a similar fashion. On the other hand, ebselen represents a new class of potent sEH phosphatase inhibitor. To our knowledge, this is the second report of direct inhibition of a phosphatase by ebselen, the first being for a hog gastric phosphatase [35]. Because we found that it did not inhibit the human alkaline phosphatase, ebselen is probably not a general phosphatase inhibitor.

*Selectivity, kinetic constants, and mechanism of ebselen inhibition*

To test the selectivity of ebselen toward sEH phosphatase, we tested its ability to inhibit Cterm-EH activity as well as human

**Table 2**
Effect of stop solutions on the assay performance.

| Stop solution | Activity (RFU)[a] | | $S/B$ | $S/N$ | $Z'$ | Stability over 30 min |
|---|---|---|---|---|---|---|
| | [E] 0 | [E] 2.1 nM | | | | |
| Control | 7 ± 1 | 124 ± 3 | 18 | 152 | 0.89 | Increase linearly |
| 100 μl of buffer | 8 ± 1 | 158 ± 5 | 20 | 178 | 0.89 | Increase linearly (similar to control) |
| 100 μl of methanol | 7 ± 2 | 62 ± 1 | 9 | 38 | 0.85 | Increase linearly (50% of control) |
| 100 μl of ethanol | 12 ± 2 | 45 ± 5 | 4 | 28 | 0.45 | Increase linearly (25% of control) |
| 100 μl of 50 mM NaOH ($pH_{final}$ 10) | 80 ± 6 | 2792 ± 138 | 35 | 450 | 0.84 | Slight increase |
| 100 μl of 0.1 M NaOH ($pH_{final}$ 12) | 71 ± 4 | 2647 ± 81 | 38 | 726 | 0.90 | Stable |
| 100 μl of 1 M NaOH ($pH_{final}$ 14) | 69 ± 3 | 1874 ± 59 | 27 | 543 | 0.90 | Stable |
| 100 μl of 30 mM SDS ($[I]_{final}$ 10 mM) | 5 ± 1 | 8 ± 1 | 2 | 8 | <0 | Stable |

[a] Results are average ± standard deviation of 16 wells.

**Table 3**
Accuracy, precision, and repeatability of AttoPhos assay for human sEH.

| | [I] (μM) | Nominal inhibition (%) | Day 1 | | Day 2 | | Day 3 | | Overall accuracy/ precision (%) |
|---|---|---|---|---|---|---|---|---|---|
| | | | Accuracy/ precision (%) | *Z* | Accuracy/ precision (%) | *Z* | Accuracy/ precision (%) | *Z* | |
| 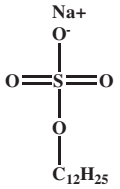 | 25 | 85 ± 1 | 100/1 | 0.5 ± 0.2 | 99/1 | 0.4 ± 0.2 | 99/1 | 0.4 ± 0.1 | 100/1 |
| | 12.5 | 67 ± 1 | 99/3 | 0.8 ± 0.1 | 100/3 | 0.6 ± 0.1 | 98/3 | 0.7 ± 0.1 | 98/2 |
| | 6.3 | 40 ± 2 | 97/3 | 0.8 ± 0.1 | 98/3 | 0.9 ± 0.1 | 95/5 | 0.8 ± 0.1 | 96/2 |
| | 3.1 | 17 ± 1 | 94/5 | 0.9 ± 0.1 | 99/8 | 0.9 ± 0.1 | 95/12 | 0.8 ± 0.1 | 90/3 |
| | 1.6 | 5 ± 1 | 81/48 | 0.9 ± 0.1 | 72/25 | 0.9 ± 0.1 | 91/30 | 0.9 ± 0.1 | 77/21 |
| $IC_{50}$ (μM) | | 9.4 ± 0.6 | 9.0 ± 1.1 | | 9.0 ± 0.3 | | 10.1 ± 1.6 | | |
| 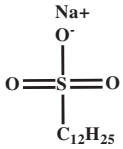 | 25 | 89 ± 1 | 99/1 | 0.3 ± 0.1 | 100/1 | 0.3 ± 0.1 | 99/2 | 0.3 ± 0.1 | 100/1 |
| | 12.5 | 78 ± 3 | 96/1 | 0.5 ± 0.1 | 100/2 | 0.6 ± 0.1 | 96/3 | 0.6 ± 0.1 | 100/1 |
| | 6.3 | 54 ± 4 | 92/3 | 0.7 ± 0.1 | 97/2 | 0.7 ± 0.1 | 95/6 | 0.7 ± 0.1 | 98/2 |
| | 3.1 | 26 ± 4 | 80/2 | 0.8 ± 0.1 | 89/6 | 0.8 ± 0.1 | 91/9 | 0.8 ± 0.1 | 96/6 |
| | 1.6 | 9 ± 6 | 63/11 | 0.8 ± 0.1 | 68/19 | 0.8 ± 0.1 | 91/17 | 0.8 ± 0.1 | 79/16 |
| $IC_{50}$ (μM) | | 6.6 ± 0.8 | 6.3 ± 0.3 | | 6.1 ± 0.3 | | 7.5 ± 1.2 | | |
| 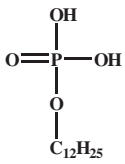 | 12.5 | 98 ± 1 | 99/1 | <0 | 99/1 | <0 | 100/1 | <0 | 98/2 |
| | 6.3 | 91 ± 1 | 99/1 | 0.1 ± 0.1 | 99/1 | 0.1 ± 0.1 | 100/1 | 0.2 ± 0.1 | 97/6 |
| | 3.1 | 70 ± 3 | 95/1 | 0.7 ± 0.1 | 100/4 | 0.7 ± 0.1 | 95/1 | 0.7 ± 0.2 | 94/5 |
| | 1.6 | 39 ± 5 | 87/2 | 0.8 ± 0.2 | 98/13 | 0.8 ± 0.2 | 86/4 | 0.8 ± 0.1 | 90/13 |
| | 0.8 | 19 ± 4 | 86/21 | 0.9 ± 0.1 | 89/26 | 0.9 ± 0.1 | 80/8 | 0.8 ± 0.1 | 69/22 |
| $IC_{50}$ (μM) | | 2.2 ± 0.3 | 1.8 ± 0.2 | | 2.3 ± 0.2 | | 2.4 ± 0.1 | | |
| *S/B* | | | 19.3 ± 0.2 | | 17.6 ± 0.3 | | 14.2 ± 0.3 | | 17 ± 3 |
| *S/N* | | | 87 ± 11 | | 87 ± 11 | | 84 ± 10 | | 86 ± 2 |
| *Z′* | | | 0.88 ± 0.02 | | 0.81 ± 0.08 | | 0.87 ± 0.05 | | 0.85 ± 0.04 |

**Table 4**
Counterscreening of positive hits.

| Structure | Name | $IC_{50}$ (μM) |
|---|---|---|
| 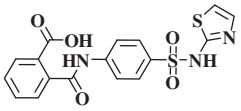 | Phthalylsulfathiazole | >100 |
| 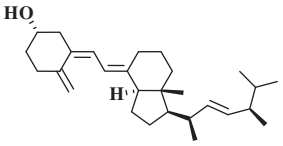 | Ergocalciferol | >100 |
| 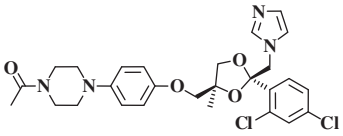 | Ketoconazole | >100 |
| 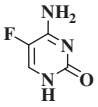 | Fluocytosine | >100 |
| 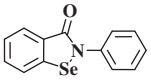 | Ebselen | 0.40 ± 0.02 |
| 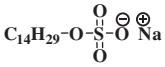 | Sodium tetradecyl sulfate | 7.0 ± 0.6 |

Potencies against Nterm-phos ($IC_{50}$) were determined with freshly made solution of the compounds in $Me_2SO$.

microsomal EH, human alkaline phosphatase, and a series of esterases and amidases [26,29]. Interestingly, we found that, in addition to Nterm-phos, ebselen also inhibits Cterm-EH but not the other enzymes tested. However, it does so with an $IC_{50}$ (2.2 ± 0.3 μM) that is fivefold higher than that observed for Nterm-phos (Table 3). To test the hypothesis that ebselen inhibition of both activities of sEH is independent, we measured the effect of ebselen on both domains of sEH expressed separately [22,26]. We found that 10 μM

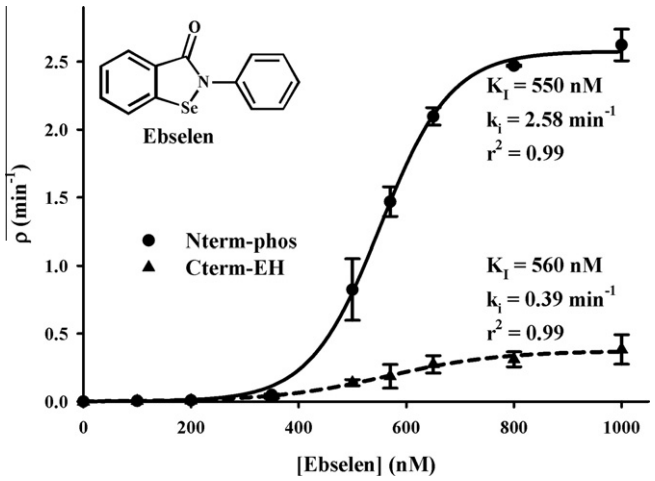


**Fig.2.** Determination of kinetic constants of Nterm-phos and Cterm-EH inhibition by ebselen using a model of irreversible inhibition [35]. The human sEH (3.3 nM) was incubated under the conditions described in the text with various concentrations of ebselen. Activities were measured at several time points (0.5 to 30 min) after inhibitor addition, by adding a saturating concentration of substrates (25 μM AttoPhos for Nterm-phos [26] and 50 μM PHOME for Cterm-EH) [29]. The initial rate of the enzyme–inhibitor complex formation (ρ) was then calculated as described [35]. The plot of ρ versus the inhibitor concentration permits the determination of the dissociation constant ($K_I$) and first-order formation rate of the covalent enzyme–inhibitor complex ($k_i$).

ebselen for 5 min did not significantly inhibit the Cterm-EH expressed alone, while the Nterm-phos expressed alone was totally inhibited by the same treatment. This result suggests that ebselen interacts only with the N-terminal domain of sEH. Furthermore, we tested whether ebselen inhibition was reversible. After incubating 20 nM human sEH with 10 μM ebselen for 15 min, we dialyzed the enzyme to remove the small molecule. After exposure to the selenium-containing compound, we were not able to recover any of the Nterm-phos or Cterm-EH activities, suggesting that ebselen chemically reacts with the human sEH. Pretreatment of the enzyme with 5 mM glutathione before exposure to 10 μM ebselen for 5 min protected the human sEH activities. The addition of glutathione to the enzyme 5 min after exposure to ebselen did not permit the recovery of the Nterm-phos activity, but 30% of the Cterm-EH activity was recovered. Taken together, these results suggest a redox mechanism, which is not surprising since ebselen is used as an antioxidant [35,36]. Interestingly, while Nterm-phos is stably and quickly inhibited by ebselen (less than a minute), Cterm-EH inhibition increases with time: its $IC_{50}$ decreased from 2.0 ± 0.3 to 0.85 ± 0.05 μM if the incubation time increased from 1 to 15 min. To support this observation we determined the kinetic constants of ebselen inhibition of Nterm-phos [26] and Cterm-EH [29] using a model of irreversible inhibition (Fig. 2) [38]. Interestingly, we observed similar dissociation constants ($K_I$) for both activities (Nterm-phos $K_I$ = 551 ± 6 nM, $n$ = 3; Cterm-EH $K_I$ = 560 ± 10 nM, $n$ = 3), while the first-order formation rate of the covalent enzyme–inhibitor complex ($k_i$) is around sevenfold faster for Nterm-phos ($k_i$ = 2.58 ± 0.05 min$^{-1}$, $n$ = 3) than for Cterm-EH ($k_i$ = 0.39 ± 0.07 min$^{-1}$, $n$ = 3). Furthermore, sigmoidal curves were obtained for both activities (Fig. 2), suggesting a cooperative or allosteric-like mechanism. Taken together these results suggest that ebselen chemically reacts with the N-terminal domain of the human sEH, rapidly inhibits Nterm-phos, and generates conformational changes leading to the slower denaturation of the enzyme and inhibition of Cterm-EH. In the mouse sEH, but not the human sEH, a cysteine residue, which is not in the active site, can allosterically inhibit the Cterm-EH activity when chemically modified [39]. More recently, the human sEH was shown to be redox regulated by 15-deoxy-Δ-prostaglandin, an electrophilic oxidant that dilates the coronary vasculature [40]. The results observed herein with ebselen are consistent with these previous observations.

In conclusion, we developed an excellent HTS assay for measuring the phosphatase activity of the human sEH that can be used to screen chemical libraries. The observed inhibition of HsEH by ebselen is intriguing. Because ebselen is an antioxidant drug that has numerous activities and targets [36,37], it is unlikely to be a monospecific Nterm-phos inhibitor in animals. Perhaps more importantly, the mode of action of ebselen suggests that the N-terminal domain of sEH contains an allosteric regulatory site for both of its catalytic activities. Nevertheless, it represents a lead for a new class of potent sEH phosphatase inhibitors that may provide valuable tools to investigate the biological role of the Nterm-phos. Toward such a goal, one will need to characterize what adduct is formed on sEH in the presence of ebselen, as well as determining if mimics of glutathione peroxidases are a new class of sEH inhibitors or if it is more specific to selenium-containing antioxidants.

## Acknowledgments

This work was partially funded by NIEHS Grant ES02710, NIEHS Superfund Basic Research Program Grant P42 ES04699, and American Asthma Foundation Grant 09-0269. B.D.H. is a George and Judy Marcus Senior Fellow of the American Asthma Foundation.

## Appendix A. Supplementary data

Supplementary data associated with this article can be found, in the online version, at http://dx.doi.org/10.1016/j.ab.2012.11.017.

## References

[1] J.W. Newman, C. Morisseau, B.D. Hammock, Epoxide hydrolases: their roles and interactions with lipid metabolism, Prog. Lipid Res. 44 (2005) 1–51.
[2] C. Morisseau, B.D. Hammock, Gerry Brooks and epoxide hydrolases: four decades to a pharmaceutical, Pest Manage. Sci. 64 (2008) 594–609.
[3] B.M. De Taeye, C. Morisseau, J. Coyle, J.W. Covington, A. Luria, J. Yang, S.B. Murphy, D.B. Friedman, B.D. Hammock, D.E. Vaughan, Expression and regulation of soluble epoxide hydrolase in adipose tissue, Obesity 18 (2010) 489–498.
[4] G.A. Gomez, C. Morisseau, B.D. Hammock, D.W. Christianson, Structure of human soluble epoxide hydrolase reveals mechanistic interferences on bifunctional catalysis in epoxide and phosphate ester hydrolysis, Biochemistry 43 (2004) 4716–4723.
[5] J.D. Imig, B.D. Hammock, Soluble epoxide hydrolase as a therapeutic target for cardiovascular diseases, Nat. Rev. Drug Discovery 8 (2009) 794–805.
[6] A. Iyer, D.P. Fairlie, J.B. Prins, B.D. Hammock, L. Brown, Inflammatory lipid mediators in adipocyte function and obesity, Nat. Rev. Endocrinol. 6 (2010) 71–82.
[7] R.H. Ingraham, R.D. Gless, H.Y. Lo, Soluble epoxide hydrolase inhibitors and their potential for treatment of multiple pathologic conditions, Curr. Med. Chem. 18 (2011) 587–603.
[8] A. Cronin, S. Mowbray, H. Dürk, S. Homburg, I. Fleming, B. Fisslthaler, F. Oesch, M. Arand, The N-terminal domain of mammalian soluble epoxide hydrolase is a phosphatase, Proc. Natl. Acad. Sci. USA 100 (2003) 1552–1557.
[9] J.W. Newman, C. Morisseau, T.R. Harris, B.D. Hammock, The soluble epoxide hydrolase encoded by EPXH2 is a bifunctional enzyme with novel lipid phosphate phosphatase activity, Proc. Natl. Acad. Sci. USA 100 (2003) 1558–1563.
[10] C. Morisseau, B. Inceoglu, K. Schmelzer, H.J. Tsai, S.L. Jinks, C.M. Hegedus, B.D. Hammock, Naturally occurring monoepoxides of eicosapentaenoic acid and docosahexaenoic acid are bioactive antihyperalgesic lipids, J. Lipid Res. 51 (2010) 3481–3490.
[11] C. Morisseau, M.H. Goodrow, D. Dowdy, J. Zheng, J.F. Greene, J.R. Sanborn, B.D. Hammock, Potent urea and carbamate inhibitors of soluble epoxide hydrolases, Proc. Natl. Acad. Sci. USA 96 (1999) 8849–8854.
[12] N. Chiamvimonvat, C.M. Ho, H.J. Tsai, B.D. Hammock, The soluble epoxide hydrolase as a pharmaceutical target for hypertension, J. Cardiovasc. Pharmacol. 50 (2007) 225–237.
[13] J.D. Imig, Targeting epoxides for organ damage in hypertension, J. Cardiovasc. Pharmacol. 56 (2010) 329–335.

[14] J.J. Iliff, J. Jia, J. Nelson, T. Goyagi, J. Klaus, N.J. Alkayed, Epoxyeicosanoid signaling in CNS function and disease, Prostaglandins Other Lipid Mediators 91 (2010) 68–84.
[15] A. Luria, C. Morisseau, H.J. Tsai, J. Yang, B. Inceoglu, B. De Taeye, S.M. Watkins, M.M. Wiest, J.B. German, B.D. Hammock, Alteration in plasma testosterone levels in male mice lacking soluble epoxide hydrolase, Am. J. Physiol. Endocrinol. Metab. 297 (2009) E375–E383.
[16] A.E. EnayetAllah, A. Luria, B. Luo, H.J. Tsai, P. Sura, B.D. Hammock, D.F. Grant, Opposite regulation of cholesterol levels by the phosphatase and hydrolase domains of soluble epoxide hydrolase, J. Biol. Chem. 283 (2008) 36592–36598.
[17] A. Oguro, K. Sakamoto, S. Suzuki, S. Imaoka, Contribution of hydrolase and phosphatase domains in soluble epoxide hydrolase to vascular endothelial growth factor expression and cell growth, Biol. Pharm. Bull. 32 (2009) 1962–1967.
[18] B. Keserü, E. Barbosa-Sicard, R.T. Schermuly, H. Tanaka, B.D. Hammock, N. Weissmann, B. Fisslthaler, I. Fleming, Hypoxia-induced pulmonary hypertension: comparison of soluble epoxide hydrolase deletion vs. inhibition, Cardiovasc. Res. 85 (2010) 232–240.
[19] H.H. Hou, B.D. Hammock, K.H. Su, C. Morisseau, Y.R. Kou, S. Imaoka, A. Oguro, S.K. Shyue, J.F. Zhao, T.S. Lee, N-terminal domain of soluble epoxide hydrolase negatively regulates the VEGF-mediated activation of endothelial nitric oxide synthase, Cardiovasc. Res. 93 (2012) 120–129.
[20] M. Fornage, E. Boerwinkle, P.A. Doris, D. Jacobs, K. Liu, N.D. Wong, Polymorphism of the soluble epoxide hydrolase is associated with coronary artery calcification in African-American subjects, Circulation 109 (2004) 335–339.
[21] K. Ohtoshi, H. Kaneto, K. Node, Y. Nakamura, T. Shiraiwa, M. Matsuhisa, Y. Yamasaki, Association of soluble epoxide hydrolase gene polymorphism with insulin resistance in type 2 diabetic patients, Biochem. Biophys. Res. Commun. 331 (2005) 347–350.
[22] B.D. Przybyla-Zawislak, P.K. Srivastava, J. Vásquez-Matías, H.W. Mohrenweiser, J.E. Maxwell, B.D. Hammock, J.A. Bradbury, A.E. Enayetallah, D.C. Zeldin, D.F. Grant, Polymorphisms in human soluble epoxide hydrolase, Mol. Pharmacol. 64 (2003) 482–490.
[23] P.K. Srivastava, V.K. Sharma, D.S. Kalonia, D.F. Grant, Polymorphisms in human soluble epoxide hydrolase: effects on enzyme activity, enzyme stability, and quaternary structure, Arch. Biochem. Biophys. 427 (2004) 164–169.
[24] C. Fava, M. Montagnana, E. Danese, P. Almgren, B. Hedblad, G. Engström, G. Berglund, P. Minuz, O. Melander, Homozygosity for the EPHX2 K55R polymorphism increases the long-term risk of ischemic stroke in men: a study in Swedes, Pharmacogenet. Genomics 20 (2010) 94–103.
[25] C. Morisseau, N.H. Schebb, H. Dong, A. Ulu, P.A. Aronov, B.D. Hammock, Role of soluble epoxide hydrolase phosphatase activity in the metabolism of lysophosphatidic acids, Biochem. Biophys. Res. Commun. 419 (2012) 796–800.
[26] K.L. Tran, P.A. Aronov, H. Tanaka, J.W. Newman, B.D. Hammock, C. Morisseau, Lipid sulfates and sulfonates are allosteric competitive inhibitors of the N-terminal phosphatase activity of the mammalian soluble epoxide hydrolase, Biochemistry 44 (2005) 12179–12187.
[27] A.E. Enayetallah, D.F. Grant, Effects of human soluble epoxide hydrolase polymorphisms on isoprenoid phosphate hydrolysis, Biochem. Biophys. Res. Commun. 341 (2006) 254–260.
[28] M.I. El-Barghouthi, A.I. Saleh, A. Ghandour, R. Ghanem, M. Zacharias, Examining the potency of suggested inhibitors for the phosphatase activity of the human soluble epoxide hydrolase by molecular dynamics simulations, J. Mol. Struct., Theochem 944 (2010) 97–104.
[29] C. Morisseau, O. Merzlikin, A. Lin, G. He, W. Feng, I. Padilla, M.S. Denison, I.N. Pessah, B.D. Hammock, Toxicology in the fast lane: application of high-throughput bioassays to detect modulation of key enzymes and receptors, Environ. Health Perspect. 117 (2009) 1867–1872.
[30] J.K. Beetham, T. Tian, B.D. Hammock, CDNA cloning and expression of a soluble epoxide hydrolase from human liver, Arch. Biochem. Biophys. 305 (1993) 197–201.
[31] R.N. Wixtrom, M.H. Silva, B.D. Hammock, Affinity purification of cytosolic epoxide hydrolase using derivatized epoxy-activated Sepharose gels, Anal. Biochem. 169 (1988) 71–80.
[32] J.H. Zhang, T.D. Chung, K.R. Oldenburg, A simple statistical parameter for use in evaluation and validation of high throughput screening assays, J. Biomol. Screen. 4 (1999) 67–73.
[33] S. Hahn, J. Achenbach, E.L. Buscató, F.M. Klingler, M. Schroeder, K. Meirer, M. Hieke, J. Heering, E. Barbosa-Sicard, F. Loehr, I. Fleming, V. Doetsch, M. Schubert-Zsilavecz, D. Steinhilber, E. Proschak, Complementary screening techniques yielded fragments that inhibit the phosphatase activity of soluble epoxide hydrolase, Chem. Med. Chem. 6 (2011) 2146–2149.
[34] K. Ogino, T. Kakihara, M. Abe, Estimation of the critical micelle concentrations and aggregation numbers of sodium alkyl sulfates by capillary-type isotachophoresis, Colloid Polym. Sci. 265 (1987) 604–612.
[35] Y. Tabuchi, T. Ogasawara, K. Furuhama, Mechanism of the inhibition of hog gastric H+, K(+)-ATPase by the seleno-organic compound ebselen, Arzneimittelforschung 44 (1994) 51–54.
[36] K. Suzuki, Anti-oxidants for therapeutic use: why are only a few drugs in clinical use?, Adv Drug Delivery Rev. 61 (2009) 287–289.
[37] K.P. Bhabak, G. Mugesh, Functional mimics of glutathione peroxidase: bioinspired synthetic antioxidants, Acc. Chem. Res. 43 (2010) 1408–1419.
[38] C. Morisseau, G. Du, J.W. Newman, B.D. Hammock, Mechanism of mammalian soluble epoxide hydrolases inhibition by chalcone oxide derivatives, Arch. Biochem. Biophys. 356 (1998) 214–228.
[39] E.C. Dietze, J. Stephens, J. Magdalou, D.M. Bender, M. Moyer, B. Fowler, B.D. Hammock, Inhibition of human and murine cytosolic epoxide hydrolase by group-selective reagents, Comp. Biochem. Physiol. B 104 (1993) 299–308.
[40] R.L. Charles, J.R. Burgoyne, M. Mayr, S.M. Weldon, N. Hubner, H. Dong, C. Morisseau, B.D. Hammock, A. Landar, P. Eaton, Redox regulation of soluble epoxide hydrolase by 15-deoxy-delta-prostaglandin J2 controls coronary hypoxic vasodilation, Circ. Res. 108 (2011) 324–334.

Prepared for Analytical Biochemistry

# Development of an HTS assay for EPHX2 phosphatase activity and screening of non-targeted libraries (supplementary material)

Christophe Morisseau,[1,*] Sunil Sahdeo,[2] Gino Cortopassi,[2] and Bruce D. Hammock[1]

[1] Department of Entomology and UCD Comprehensive Cancer Center, [2] School of Veterinary Medicine, Department of Molecular Biosciences, One Shields Avenue, University of California, Davis C.A. 95616, U.S.A.

Running title: sEH phosphatase HTS assay

Address correspondence to: Christophe Morisseau
Department of Entomology
University of California at Davis
One Shields Avenue, Davis, CA 95616.
Tel: 530 752 6571
Fax: 530-751-1537
E-mail: chmorisseau@ucdavis.edu

**Table S1: comparison of the assay in 96- and 384-well plates**

| | 96-well plates (n = 9) | 384-well plates (n = 4) |
|---|---|---|
| S/B | 17 ± 3 | 66 ± 8 |
| S/N | 86 ± 2 | 286 ± 39 |
| Z' | 0.85 ± 0.04 | 0.77 ± 0.10 |
| | $IC_{50}$ (µM) | |
| 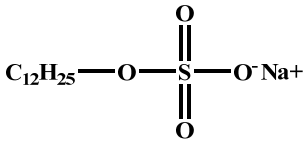 | 9.4 ± 0.6 | 9.0 ± 2.2 |
| 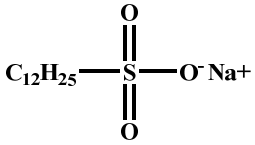 | 6.6 ± 0.8 | 5.5 ± 1.3 |
| 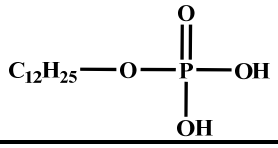 | 2.2 ± 0.3 | 1.8 ± 0.9 |

**Figure S1:** results of the checkerboard assay for the optimization of [E] and [S] after 60 min of reaction at room temperature. **A**: effect on substrate turn over; **B**: effect on $r^2$; **C**: effect on signal to background ratio (S/B); **D**: effect on signal to noise ratio (S/N); **E**: effect on Z'.

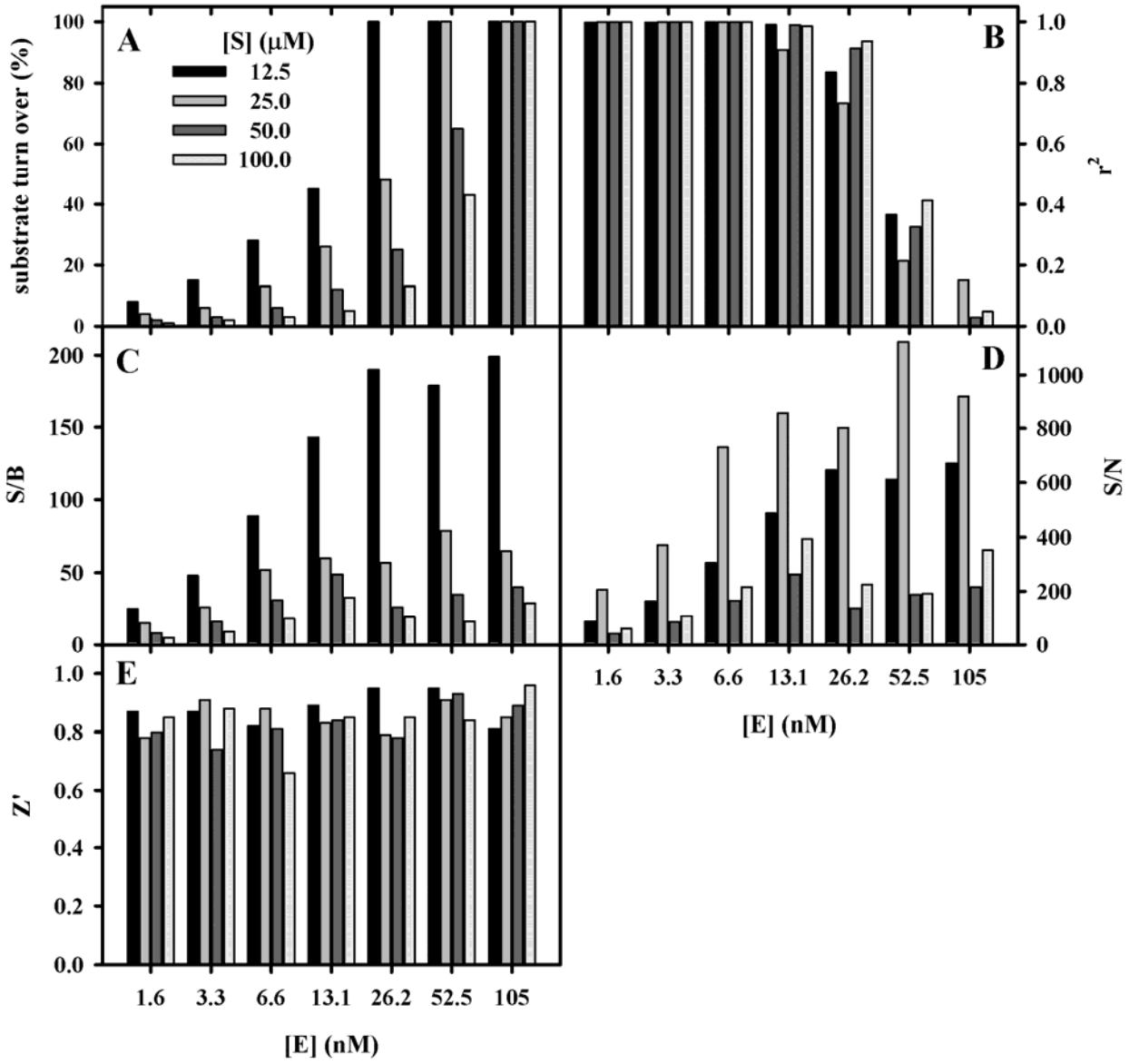

**Figure S2:** The reaction of Attophos with sEH, and subsequent alkalinization to produce the highly fluorescent phenolate product.

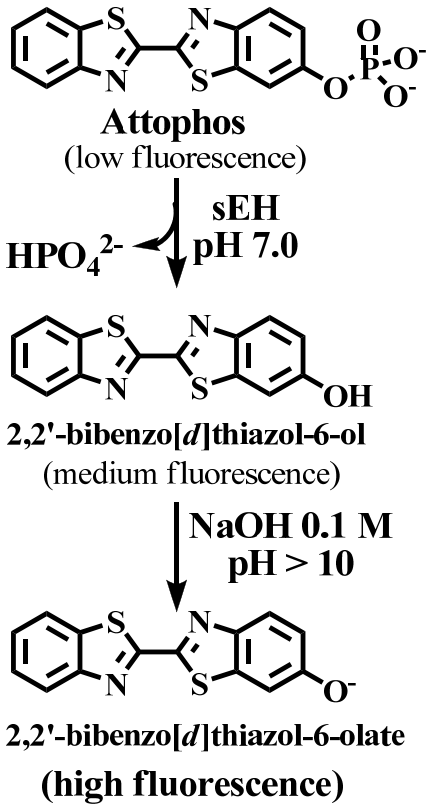

**Figure S3**: comparison of the fluorescent signal from the enzymatic reaction obtained before and after the addition of 100 μL of NaOH 0.1M as stop solution.

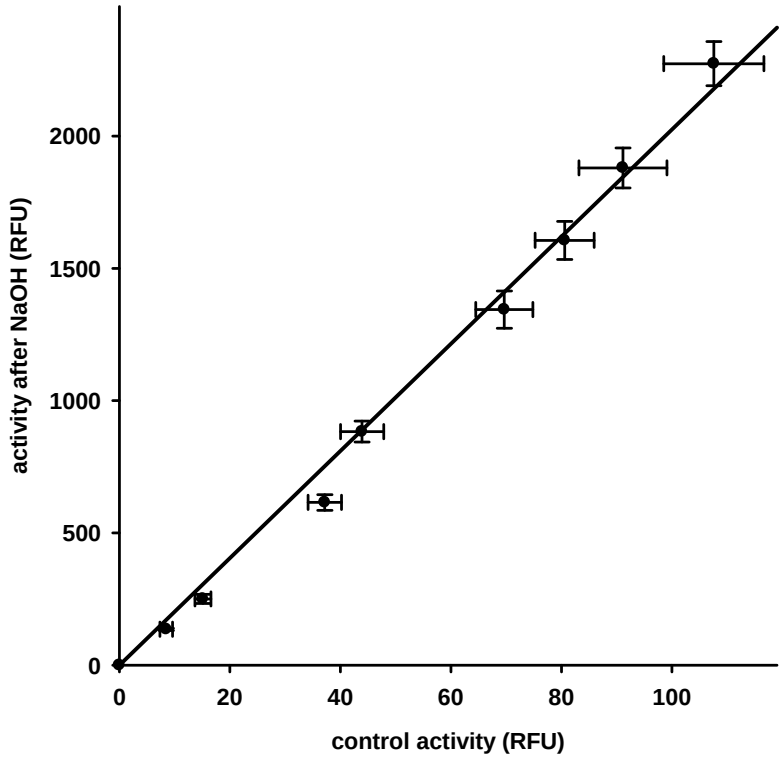

**Figure S4**: Effect of Nterm-phos inhibition on Z value.

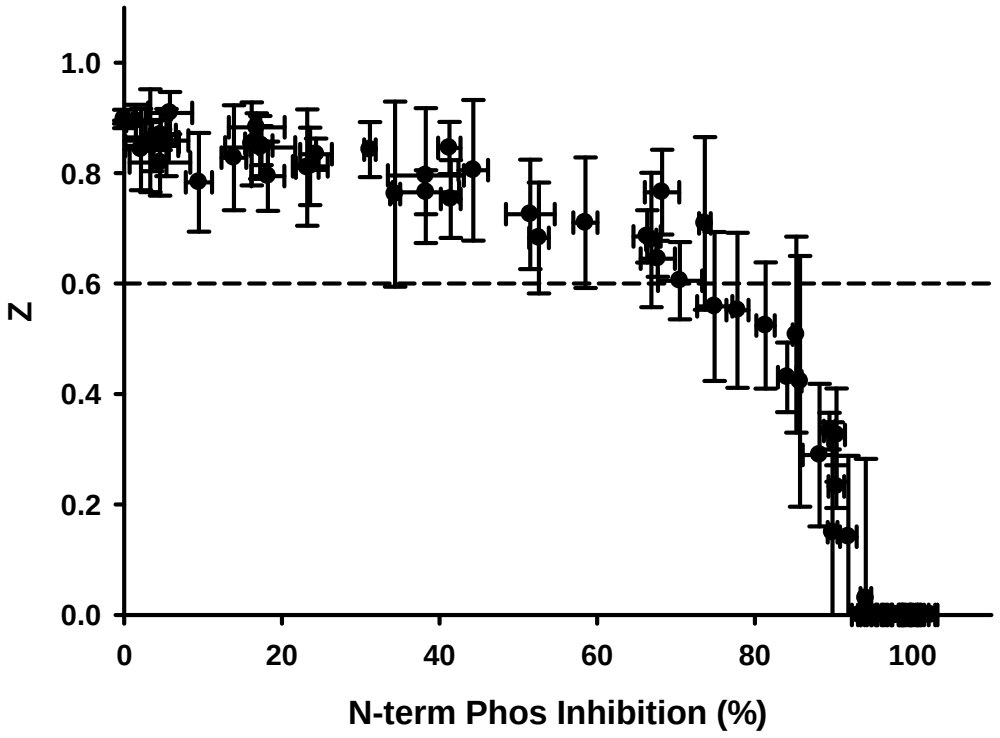

**Figure S5**: Primary screening results of the Pharmacon library. Percent of Nterm-phos inhibition for each compound tested at 10 μM. Compounds that gave more than 80% inhibition (dashed line) were selected for secondary screening.